Talanta 137 (2015) 156–160

Contents lists available at ScienceDirect

Talanta

journal homepage: www.elsevier.com/locate/talanta

Short communication

Real-time fluorescence assays of alkaline phosphatase and ATP sulfurylase activities based on a novel PPi fluorescent probe

Xiaobo Wang, Zhiyang Zhang, Xiaoyan Ma, Jinghan Wen, Zhirong Geng*, Zhilin Wang*

State Key Laboratory of Coordination Chemistry, School of Chemistry and Chemical Engineering, Collaborative Innovation Center of Advanced Microstructures, Nanjing University, Nanjing 210093, PR China

ARTICLE INFO

Article history:
Received 20 November 2014
Received in revised form
17 January 2015
Accepted 21 January 2015
Available online 2 February 2015

Keywords:
PPi
Fluorescent probe
Alkaline phosphatase
ATP sulfurylase
Real-time fluorescence assay

ABSTRACT

An anthracene-armed tetraaza macrocyclic fluorescent probe 3-(9-anthrylmethyl)-3,6,9,15-tetraazabicyclo[9.3.1]pentadeca-1(15),11,13-triene(L) for detecting Zn^{2+} in aqueous medium was synthesized. L–Zn^{2+} complex, showed selectivity toward pyrophosphate ion (PPi) by quenching the fluorescence in aqueous HEPES buffer (pH 7.4). Furthermore, L–Zn^{2+} was also used to set up a real-time fluorescence assay for monitoring enzyme activities of alkaline phosphatase (ALP) and adenosine triphosphate sulfurylase (ATPS). In the presence of ALP inhibitor Na_3VO_4 and ATPS inhibitor chlorate, two enzymes activities decreased obviously, respectively.

1. Introduction

Alkaline phosphatase (EC 3.1.3.1) is one of the most commonly enzymes in various mammals and has long been identified as an important biomarker in clinical practice because its levels are elevated in both serum and synovial fluid from rheumatoid arthritis (RA) patients [1–3]. ALP levels have been positively correlated with RA activity [1,4,5]. Differently, serum ALP activity decreases in patients with calcium pyrophosphate deposition disease and hypophosphatasis [6–8]. Besides, ALP activity is often associated with bone, liver dysfunction, breast cancer, diabetes, leukemia, *etc* [9–15]. ATP sulfurylase (ATPS, EC 2.7.7.4), which is ubiquitous in all kinds of organisms including mammalian species, catalyzes a key reaction in the global sulfur cycle by reversibly converting SO_4^{2-} with ATP to PPi and adenosine 5′-phosphosulfate (APS) [16,17]. Then APS is phosphorylated by APS kinase on it's 3′-hydroxyl group to yield 3′-phosphoadenosine 5′-phosphosulfate (PAPS) as the activated form of sulfate in the dissimilatory process and in the assimilatory process of plants, algae, most bacteria and mammalian species [17–23]. In the animal kingdom, ATPS activities are associated with severe connective tissue abnormalities such as spondyloepimetaphyseal dysplasia in humans and brachymorphism in mice [24]. Moreover, ATPS activity is inhibited potently and PAPS accumulates in bipolar disorder (manic depressive disease) patients treated with lithium. In contrast, PAPS level plummets obviously in the presence of chlorate, a widely used cell-permeable inhibitor of mammalian and yeast ATPS activity. In other words, administration of chlorate can reduce lithium-induced intracellular PAPS accumulation and lithium toxicity [25]. Thus, how to simply and exactly determine ALP and ATPS activities has been highlighted in clinical diagnoses. Regardless, there remain no accurate, high-throughout, quantitative and simple methods for screening inhibitors of ATPS based on fluorometric assay hitherto.

Currently, real-time fluorescence enzyme assay, which is convenient and high-performance attracted wide attention. However, only a few real-time fluorescence ALP assays have been successfully established, while those for ATPS are still lacking [26]. Thereby motivated, we herein established a real-time fluorescence assay of ALP and ATPS activities by employing PPi as substrate.

2. Experimental

2.1. Apparatus and reagents

All the starting materials were of reagent quality and were obtained from commercial sources without further purification. Alkaline phosphatase (EC 3.1.3.1), adenosine triphosphate sulfurylase (ATPS, EC 2.7.7.4) and Adenosine 5′-phosphosulfate sodium salt (APS) were purchased from Sigma-Aldrich Co., Ltd. L-phenylalanine and $Na_3VO_4 \cdot 10H_2O$ were purchased from J&K scientific Ltd. ALP kit purchased from Nanjing KeyGEN Biotech. Co., Ltd. (substrate is disodium phenyl phosphate). All the emission spectra were obtained

* Corresponding authors. Tel.: +86 25 83686082; fax: +86 25 83317761.
E-mail addresses: gengzr@nju.edu.cn (Z. Geng), wangzl@nju.edu.cn (Z. Wang).

http://dx.doi.org/10.1016/j.talanta.2015.01.028
0039-9140/

using a PerkinElmer LS 55 fluorescence spectrometer. The electrospray ionization mass spectra were determined by a LCQ Fleet ThermoFisher mass spectrometer. ^{1}H NMR and ^{13}C NMR spectra in $CDCl_3$ were measured on a Bruker DRX-500 spectrometer at 25 ± 1 °C. The pH values of sample solutions were monitored by a PHS-3 system. The temperature was controlled by a LAUDA E100 circulating water pump in fluorescence titration.

2.2. Synthesis of probe L

The same method was adopted to synthesize the compound **1** according to literature [27–29]. Then 9-(chloromethyl) anthracene (227 mg, 1 mmol) in 40 mL of $CHCl_3$ was added to a 200 mL $CHCl_3$ solution of 1 (618 mg, 3 mmol) and Et_3N (102 mg, 1 mmol). The resulting mixture was then heated at 60 °C and stirred for 2 h under N_2 ambient. After being cooled to room temperature, the obtained mixture was washed with 1 MNaOH solution (20 mL × 3) and then with redistilled water (30 mL × 3). The organic layer was dried over anhydrous sodium sulfate overnight and evaporated to give the solid crude product. The residue was purified over column chromatography and eluted with a gradient of chloroform to methanol (12:1, v/v), yielding the product L (Scheme 1) as a yellow solid (210 mg, 53%). ESI–MS (CH_3CN): calcd for $C_{26}H_{28}N_4$ [L+H$^+$] 397.23, found 397.42; ^{1}H NMR (500 MHz, DMSO-d_6) δ 8.78 (d, *J*=8.8, 2*H*), 8.58 (s, 1*H*), 8.09 (d, *J*=8.3, 2*H*), 7.63 (m, 2*H*), 7.54 (d, *J*=7.9, 2*H*), 7.52 (m, 1*H*), 7.02 (dd, *J*=7.2, 3.7, 2*H*), 4.77 (s, 2*H*), 3.86 (s, 2*H*), 3.68 (s, 2*H*), 2.73 (t, *J*=5.1, 2*H*), 2.62 (m, 2*H*); ^{13}C NMR (125 MHz, DMSO-d_6) δC 136.86, 131.52, 131.40, 131.19, 129.25, 127.71, 126.00, 125.88, 125.48, 120.13, 119.61, 60.85, 54.89, 53.90, 53.50, 49.79, 49.72, 48.51 ppm.

2.3. Solution preparation

Stock solutions containing metal ions (20 mM, NaCl, KCl, $CaCl_2$, $MgCl_2$, $ZnCl_2$, $CuCl_2$, $Fe(NO_3)_3$, $FeCl_2$, $CoCl_2$, $NiCl_2$, $CdCl_2$, $Pb(NO_3)_2$, $MnCl_2$, $HgCl_2$) were prepared in deionized water. Stock solution of L was prepared by dissolving L in 50 mM HEPES buffer (containing 5% DMSO, pH 7.4). The pH value was adjusted by a PHS-3 system. Stock solutions containing anions (20 mM, NaF, NaCl, KBr, KI, Na_2CO_3, $NaHCO_3$, Na_2SO_4, Na_2S, Na_2SO_3, Na_3PO_4, Na_2HPO_4, NaH_2PO_4, adenosine 5′-triphosphate disodium salt hydrate, adenosine-5′-diphosphate disodium salt hydrate, adenosine 5′-monophosphoric acid disodium salt, $Na_4P_2O_7$) was prepared in deionized water.

2.4. Assays of ALP and ATPS activities

Different amounts of ALP (50, 100, 200, 300, 400, 500 and 600 mU, respectively) were added to a solution of L (10 μM), Zn^{2+} (10 μM), 10 μM $MgCl_2$ and PPi (10 μM) in Tris–HCl buffer (20 mM, pH 7.4) at 37 °C. The total volume of mixture is 2 mL. Emission intensity changes at 418 nm were monitored in real time. The temperature was accurately controlled by a circulating water pump.

The conditions for detecting ATPS activity are similar to ALP. Different amounts of ATPS (0, 12.5, 25, 75 and 100 mU, respectively) were added to a solution of L (10 μM), Zn^{2+} (10 μM), PPi (10 μM) 10 μM $MgCl_2$ and APS (10 μM) in Tris–HCl buffer (20 mM, pH 7.4) at 37 °C. The total volume of mixture is 2 mL.

2.5. ALP and ATPS inhibition assays

Different amounts of the ALP inhibitor Na_3VO_4 (0, 10, 15, 25 and 50 μM) were added to the pre-prepared solution containing L (10 μM), Zn^{2+} (10 μM), 10 μM $MgCl_2$ and PPi (10 μM) in Tris–HCl buffer (20 mM, pH 7.4) at 37 °C. The total volume of mixture is 2 mL. Then added ALP 150 mU/mL quickly, and real-time emission spectral changes of L at 418 nm were monitored.

Similarly, different amounts of the ATPS inhibitors (0, 100, 200, 500, 1000 and 2000 μM for phenylalanine; 250, 500, 1000, 1500 and 2000 μM for $KClO_3$) were added to the pre-prepared solution containing L (10 μM), Zn^{2+} (10 μM), 10 μM $MgCl_2$, PPi (10 μM) and APS (10 μM) in Tris–HCl buffer (20 mM, pH 7.4) at 37 °C. The total volume of mixture is 2 mL. Then real-time emission spectral changes of L at 418 nm were monitored after quickly added ATPS 50 mU/mL.

3. Results and discussion

3.1. Zn^{2+} sensing

Fig. 1(a) shows the L fluorescence emission intensity in the presence or absence of different metal ions in HEPES buffer (50 mM, pH 7.4). L showed a very weak fluorescence (OFF state) at 418 nm, the characteristic anthracene monomer emission upon excitation (368 nm), due to an effective photoinduced electron transfer (PET) process. Add 1 equiv. of Na^+, K^+, Ca^{2+}, Mg^{2+}, Fe^{2+}, Fe^{3+}, Cd^{2+}, Cr^{3+}, Pb^{2+}, Co^{2+}, Ni^{2+}, and Mn^{2+} did not change the fluorescence intensity of L (20 μM) at 418 nm, while adding Cu^{2+} and Hg^{2+} slightly quenched the fluorescence. However, the fluorescence of L enhanced (ON state) upon the addition of Zn^{2+} (1 equiv.). Besides, competitive experiments were carried out by subsequently adding 10 equiv. of the biologically abundant metal ions (Ca^{2+}, Na^+, Mg^{2+}) to buffer which already contained L and Zn^{2+}, and the Zn^{2+}-specific amplified fluorescence of L was still unaffected. Additionally, as shown in Fig. 1(b), the fluorescence intensity rises linearly with increasing concentration of Zn^{2+} (2–20 μM, linearly dependent coefficient: R^2=0.998. Fig. S5), so the limit of detection (LOD) was 1.1 μM [30–32]. The enhancement factor reached 10 at the [Zn^{2+}]/[L] ratio of 1:1, and the fluorescence unchanged at higher [Zn^{2+}], suggesting a 1:1 stoichiometry for the L–Zn^{2+} complex (Fig. 1(b), inset). Job's plot with fluorescence titrations exhibited a maximum at about 0.5 mol fraction (Fig. S6), verifying the 1:1 binding stoichiometry between L and Zn^{2+}. Furthermore, the ESI–MS peaks at *m*/*z* 519.50 and 495.50 correspond to [ZnL+CH_3CN+H_2O]$^+$ and [Zn(L–H)+2H_2O]$^+$, respectively, which are consistent with the calculated isotope results (Fig. S7). From the fluorescence titration, the association constant of L with Zn^{2+} is observed to be 1.96 × 10^5 M^{-1} (Fig. S8).

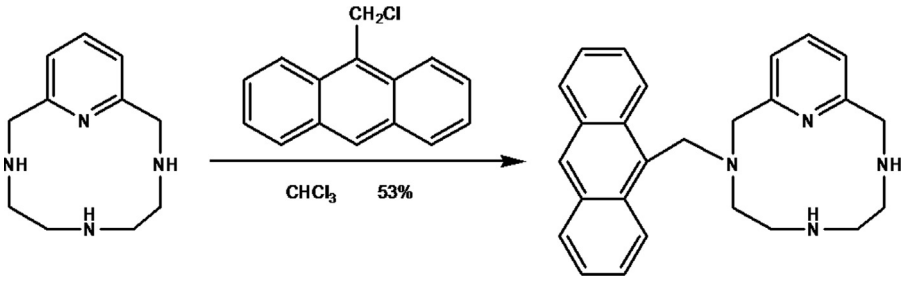

Scheme 1. Synthesis of L.

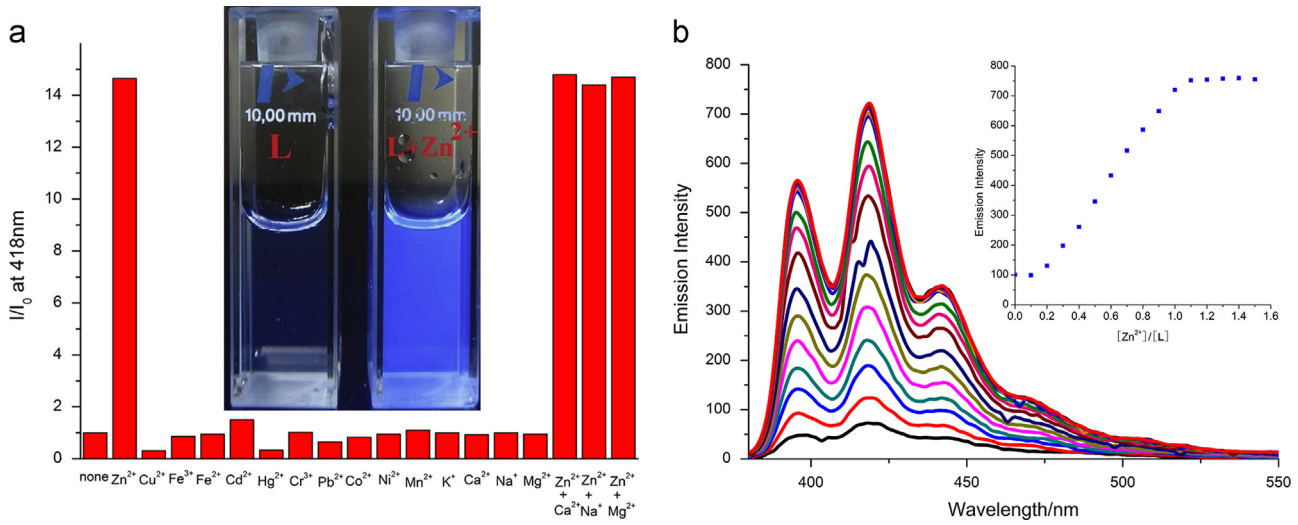

Fig. 1. (a) Histogram of I/I_0 at 418 nm induced by 1 equiv. of different metal ions and 10 equiv. of Ca^{2+}, Na^{+} and Mg^{2+} in HEPES buffer (5% DMSO, 50 mM, pH 7.4), [L]=20 μM. Inset: fluorescence color change of L (20 μM) in the absence and presence of Zn^{2+} (1 equiv.). (b) Emission spectra of 20 μM L on addition of Zn^{2+} (0–20 μM) in HEPES buffer. Inset: Fluorescence intensity *vs*. mole ratio of Zn^{2+} added to L. λ_{ex}=368 nm.

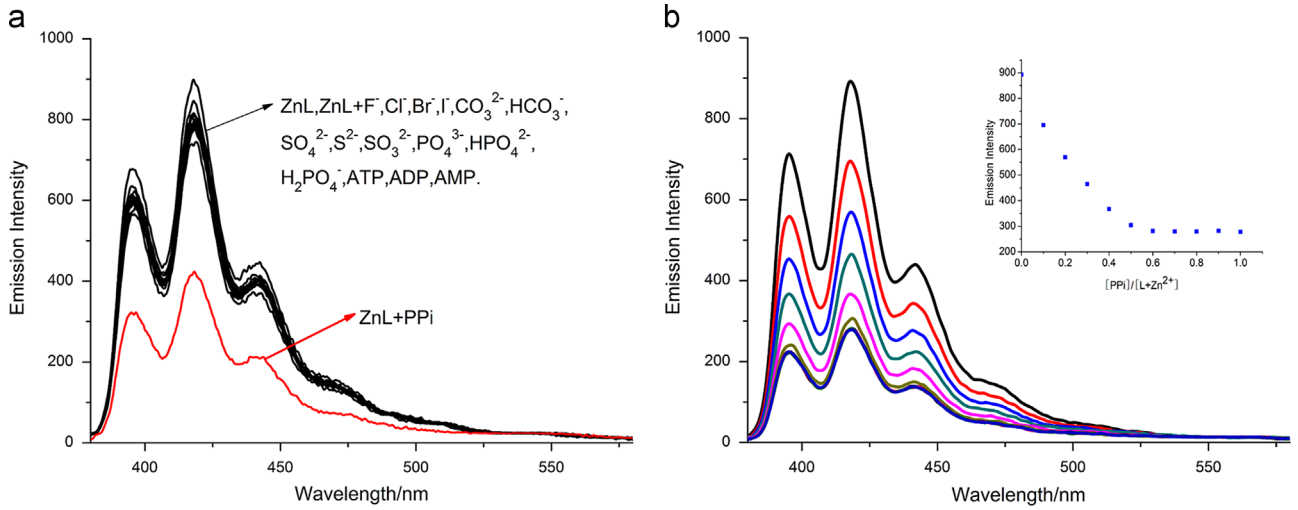

Fig. 2. (a) Fluorescence changes of L–Zn^{2+} (20 μM) upon the addition of different anions (1 equiv. as sodium salts) in 50 mM HEPES (5% DMSO, pH 7.4). (b) Emission spectra of L–Zn^{2+} in 50 mM HEPES (5% DMSO, pH 7.4) with increasing concentration of PPi (0–10 μM). The concentration of L–Zn^{2+} was 20 μM. Inset: Fluorescent intensity at 418 nm *vs*. different PPi concentrations. λ_{ex}=368 nm.

3.2. *Selectivity of L–Zn^{2+} toward PPi*

The fluorescence responses of L–Zn^{2+} towards anions, Such as F^-, Cl^-, Br^-, I^-, CO_3^{2-}, HCO_3^-, SO_4^{2-}, S^{2-}, SO_3^{2-}, PO_4^{3-}, HPO_4^{2-}, $H_2PO_4^-$, ATP, ADP, AMP and PPi were investigated in neutral HEPES buffer (Fig. 2(a)). Only PPi reduced the fluorescence intensity to 44%. The stoichiometry plot (Fig. 2(b)) analysis of the fluorescence titration profile of L–Zn^{2+} (20 μM) revealed a 2:1 stoichiometry between L–Zn^{2+} and PPi. The formation of a 2:1 complex was further supported by an ESI–MS (Fig. S9), peak at *m*/*z* 1097.25, corresponding to $[(ZnL)_2+PPi+H]^+$. In addition, the receptor L–Zn^{2+} has a detection limit of 1.1×10^{-7} M for PPi (Fig. S10).

3.3. *Real-time fluorescence assays of ALP and ATPS activities using L–Zn^{2+}*

Moreover, L–$Zn^{2+}$was used to set up a real-time fluorescence assay for monitoring the activities of PPi-relevant enzymes, such as ALP and ATPS (Fig. 3(a)). In this study, after the ALP from bovine intestinal mucosa was added rapidly, fluorescence intensity at 418 nm was monitored as a function of time at 37 °C. All the fluorescence intensities at 418 nm recover to the value absence of PPi and remained thereafter when PPi was consumed by the ALP. Importantly, the recovery rates of emission intensities differed significantly when ALP amount varied. At higher ALP concentrations, the emission intensity increased more quickly (Fig. 3(b)). The relationship between ALP activities and fluorescence intensities at 418 nm can be expressed as $I/I_0=1.007+0.00182[C_{ALP}$ (mU/mL)], $R^2=0.982$ (Fig. S11). In clinical diagnoses, ALP activity has been typically measured by utilizing all kinds of commercially available kits, which employ substrates such as disodium phenyl phosphate, *p*-nitrophenyl phosphate, *p*-aminophenyl phosphate, and 4-methylumbellyferyl phosphate [33–36]. Disodium phenyl phosphate are hydrolyzed by ALP to produce phenol. Then phenol was oxidized to red benzoquinone by potassium ferricyanide in the presence of 4-aminoantipyrine under alkaline conditions. Thus activity of ALP can be determined by measuring the absorbance of benzoquinone at wavelength of 520 nm. Herein, 3 groups of ALP concentration (between 0 and 300 U/L) were determined by ALP kit and real-time fluorescence assay, respectively (Fig. S12). The result indicated that our proposed method is reliable for clinical diagnosis.

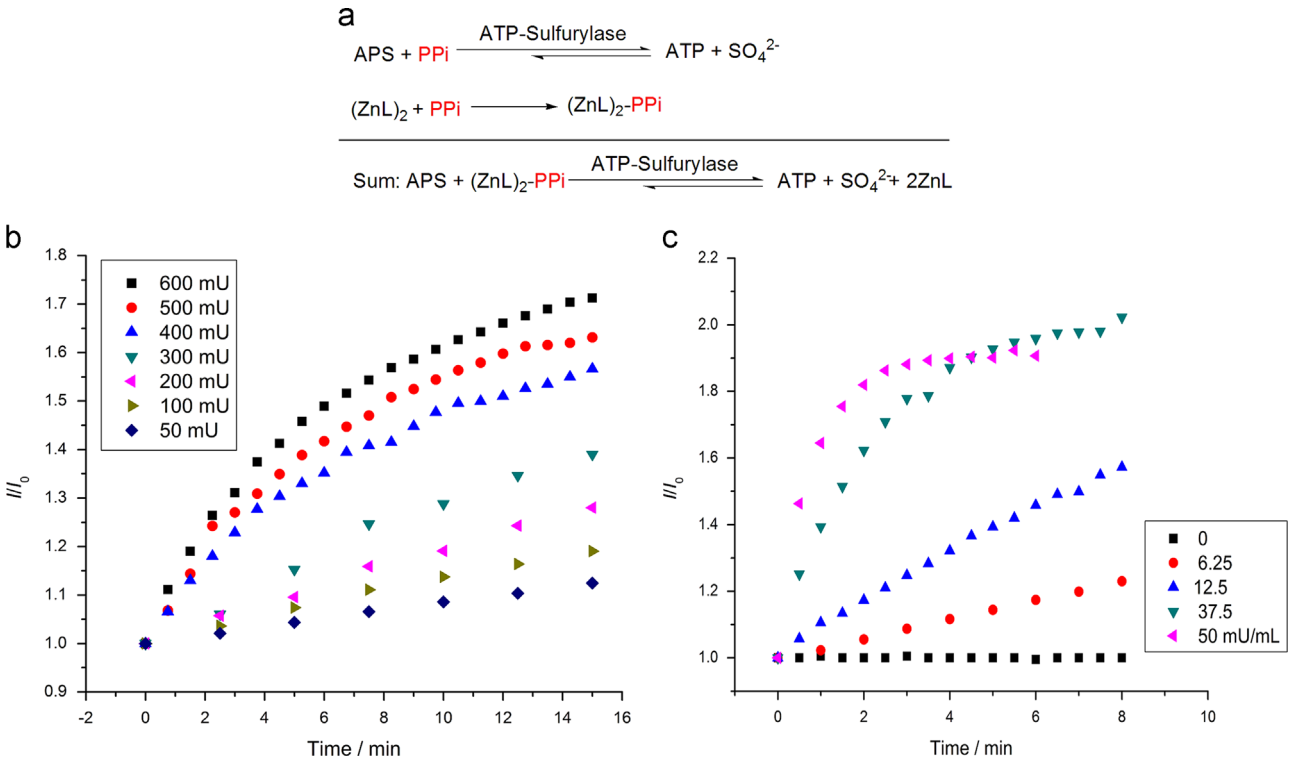

Fig. 3. (a) Mechanism of ATPS assay monitored by L–Zn^{2+}. (b) Fluorescence response of L–Zn^{2+} (10 μM) as a result of the enzymatic conversion of PPi to Pi with various concentrations of ALP at 37 °C in 20 mM Tris–HCl (5% CH_3CN, pH 7.4). (c) Fluorescence response of L–Zn^{2+} (10 μM) as a result of the enzymatic conversion of PPi to ATP with various units of ATPS at 37 °C in 20 mM Tris–HCl (5% CH_3CN, pH 7.4).

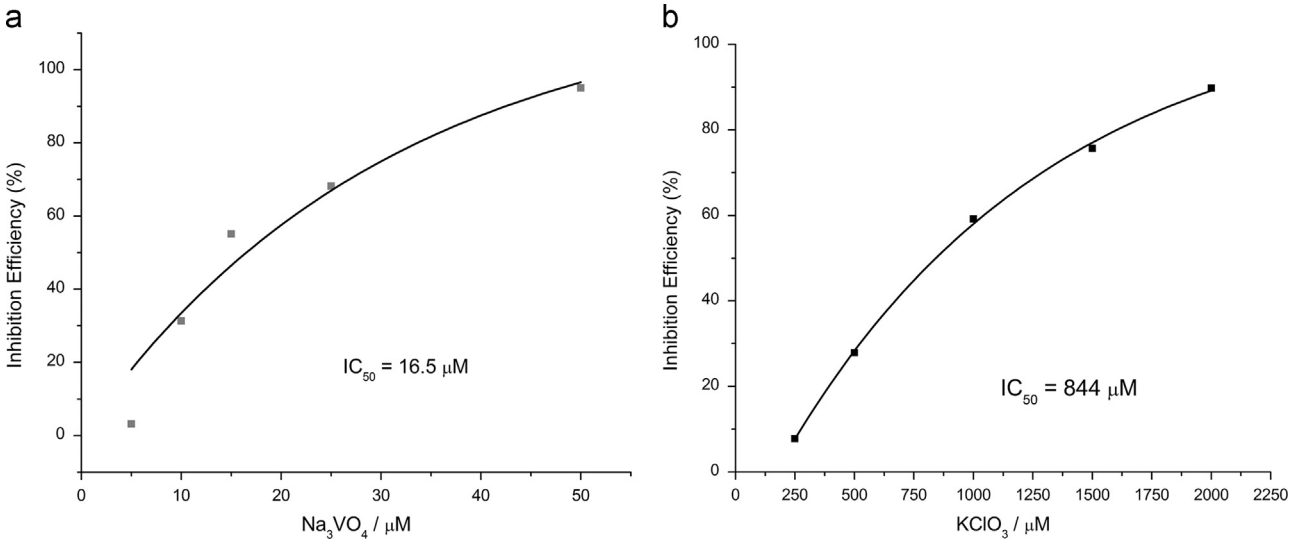

Fig. 4. (a) Plot of the inhibition efficiency *vs.* Na_3VO_4 concentration. Conditions: 20 mM Tris–HCl (pH 7.4), 10 μM L–Zn^{2+}, 10 μM PPi, 10 μM $MgCl_2$, 10 μM APS, 150 mU/mL ALP, 37 °C, 7.5 min. (b) Plot of the inhibition efficiency *vs.* $KClO_3$ concentration. Conditions: 20 mM Tris–HCl (pH 7.4), 10 μM L–Zn^{2+}, 10 μM PPi, 10 μM $MgCl_2$, 10 μM APS, 50 mU/mL ATPS, 37 °C, 3 min.

Existing in most plants and microbial cells, ATPS can catalyze the reversible reaction between PPi and ATP. Herein different amounts of ATPS were added into pre-prepared solutions containing 20 mM Tris–HCl (5% CH_3CN, pH 7.4), 10 μM L–Zn^{2+}, 10 μM $MgCl_2$, 10 μM $Na_4P_2O_7$ and 10 μM APS at 37 °C. As shown in Fig. 3(c), the recovery of fluorescence indicates PPi is consumed with elapsed time. Since the reaction was reversible, the fluorescence intensity was only recovered to about 80% of the initial one. Apparently, the emission intensity increased more quickly at higher ATPS concentrations. Within 2 min of reaction, the intensity ratios I/I_0 at 418 nm were linearly related with ATPS concentrations ranging from 0 to 50 mU/mL (Fig. S13), following the equation of $I/I_0 = 0.973 + 0.017$ [(C_{ATPS} (mU/mL)], $R^2 = 0.999$. Hence, L–Zn^{2+} can potentially be used for the real-time fluorescence monitoring of ATPS assay, although the conversion between PPi and ATP was reversible. This is the first attempt using PPi fluorescent probe for real-time monitoring of ATPS activity.

3.4. ALP and ATPS inhibition assays

Furthermore, our assay could also be used to estimate the inhibitory effects of ALP and ATPS inhibitors. Inhibition efficiency (IE) was defined by equation (I) (see SI). Na_3VO_4, a well-known inhibitor for

ALP, was tested. As shown in Fig. 4(a), elevating Na_3VO_4 concentration is conducive to the inhibition. The IC_{50} value of Na_3VO_4 toward ALP was calculated to be 16.5 μM, being lower than those (245 μM and 54.7 μM) reported by Yu et al. [37,38]. Therefore, our fluorescence system can be applied to screen highly effective inhibitors toward ALP. Phenylalanine, as an inhibitor of brain ATPS, exerted no inhibitory effect in our fluorescence system. In contrast, chlorate, a widely used cell-permeable ATPS inhibitor, was testified have a moderate inhibitory effect with the IC_{50} value of 844 μM (Fig. 4(b)).

4. Conclusion

An anthracene-armed tetraaza macrocyclic compound L was prepared as a turn-"ON" chemosensor for Zn^{2+} over other cations, and this turn-"ON" species showed selectivity toward PPi over competing anions like ATP, ADP, AMP and Pi *via* fluorescence turn-"OFF" in neutral HEPES buffer. Then, using PPi as substrate, L–Zn^{2+} functioned well for real-time fluorescence monitoring of PPase, ALP and ATPS activities. Furthermore, ALP inhibitor Na_3VO_4 and ATPS inhibitor $KClO_3$ had significant and moderate inhibitory effect on ALP and ATPS activities, respectively. Thus, our fluorescence system can be used to monitor ALP and ATPS activities as well as to screen potentially eligible ALP and ATPS inhibitors.

Acknowledgements

This work is supported by the National Basic Research Program of China (2013CB922102), the National Natural Science Foundation of China (nos. 21275072, 21201101 and 21475059) and the Natural Science Foundation of Jiangsu Province (BK20130560).

Appendix A. Supporting information

Supplementary data associated with this article can be found in the online version at http://dx.doi.org/10.1016/j.talanta.2015.01.028.

References

[1] Y. Nanke, H. Kotake, N. Kamatani, Clin. Rheumatol. 21 (2002) 198–202.
[2] A. Doube, J. Davies, M. Davis, P.J. Maddison, Ann. Rheum. Dis. 48 (1989) 368–371.
[3] R.J. Spooner, D.H. Smith, D. Bedford, P.R. Beck, J. Clin. Pathol. 35 (1982) 638–641.
[4] M.A. Cimmino, L. Buffrini, G. Barisone, H.G. Goll, G. Oremek, Z. Rheumatol. 48 (1990) 143–146.
[5] A. Akesson, K. Berglund, M. Karlsson, Scand. J. Rheumatol. 9 (1980) 81–88.
[6] G. Filippou, E. Filippucci, M. Tardella, L. Bertoldi, M.D. Carto, A. Adinolfi, W. Grassi, B. Frediani, Ann. Rheum. Dis. 72 (2013) 1836–1839.
[7] M. Doherty, C. Belcher, M. Regan, A. Jones, J. Ledingham, Ann. Rheum. Dis. 55 (1996) 432–436.
[8] R.A. Terkeltaub, Am. J. Physiol. Cell Physiol. 281 (2001) C1–C11.
[9] K. Ooi, K. Shiraki, Y. Morishita, T. Nobori, J. Clin. Lab. Anal. 21 (2007) 133–139.
[10] R.E. Gyurcsanyi, A. Bereczki, G. Nagy, M.R. Neuman, E. Lindner, Analyst 127 (2002) 235–240.
[11] R.H. Christenson, Clin. Biochem. 30 (1997) 573–593.
[12] R. Sood, Textbook of Medical Laboratory Technology, Jaypee Brothers Publishers, Noida, India, 2006.
[13] H. Jiang, X. Wang, Anal. Chem. 84 (2012) 6986–6993.
[14] J. Wang, K. Wang, B. Bartling, C. Liu, Sensors 9 (2009) 8709–8721.
[15] Y. Lin, K.S. Schanze, Anal. Chem. 80 (2008) 8605–8612.
[16] J. Herrmann, G.E. Ravilious, S.E. Mckinney, C.S. Westfall, S.G. Lee, P. Baraniecka, M. Giovannetti, S. Kopriva, H.B. Krishnan, J.M. Jez, J. Biol. Chem. 289 (2014) 10919–10929.
[17] A. Koprivova, M. Giovannetti, P. Baraniecka, B.-R. Lee, C. Grondin, O. Loudet, S. Kopriva, Plant Physiol. 163 (2013) 1133–1141.
[18] E. Hanna, I.J. Macrae, D.C. Medina, A.J. Fisher, I.H. Segel, Arch. Biochem. Biophys. 406 (2002) 275–288.
[19] Y. Inagaki, W.F. Doolittle, S.L. Baldauf, A. Roger, Curr. Biol. 12 (2002) 772–776.
[20] H. Li, A. Deyrup, J.R. Mesch, M. Domowicz, A.K. Konstantinidis, N.B. Schwartz, J. Biol. Chem. 270 (1995) 29453–29459.
[21] G.E. Ravilious, J. Herrmann, S.G. Lee, C.S. Westfall, J.M. Jez, Biosci. Rep. 33 (2013) 585–591.
[22] G.E. Ravilious, J.M. Jez, J. Biol. Chem. 287 (2012) 30385–30394.
[23] E.B. Lansdon, A.J. Fisher, I.H. Segel, Biochemistry 43 (2004) 4356–4365.
[24] N. Sekulic, M. Konrad, A. Lavie., J. Biol. Chem. 282 (2007) 22112–22121.
[25] B.D. Spiegelberg, J. dela Cruz, T.H. Law, J.D. York, J. Biol. Chem. 280 (2005) 5400–5405.
[26] P. Das, N.B. Chandar, S. Chourey, H. Agarwalla, B. Ganguly, A. Das, Inorg. Chem. 52 (2013) 11034–11041.
[27] H. Koyama, T. Yoshino, Bull. Chem. Soc. Jpn. 45 (1972) 481–484.
[28] X. Zhang, WO Pat. 97/13763, 1997.
[29] G.E. Kiefer, J. Simon, J.R. Garlich, WO Pat. 94/26754, 1994.
[30] P. Li, T. Xie, N. Fan, K. Li, B. Tang, Chem. Commun. 48 (2011) 2077–2079.
[31] Z. Mao, L. Hu, X. Dong, C. Zhong, B.-F. Liu, Z. Liu, Anal. Chem. 86 (2014) 6548–6554.
[32] D. Yu, F. Huang, S. Ding, G. Feng, Anal. Chem. 86 (2014) 8835–8841.
[33] H.J. Kim, H.B. Zhao, H. Kitaura, S. Bhattacharyya, J.A. Brewer, L.J. Muglia, F.P. Ross, S.L. Teitelbaum, J. Clin. Invest. 116 (2006) 2152–2160.
[34] R.B.R. Goncalves, R.P.M. Furriel, J.A. Jorge, F.A. Leone, Mol. Cell. Biochem. 241 (2002) 69–79.
[35] C.G. Bauer, A.V. Eremenko, E. EhrentreichForster, F.F. Bier, A. Makower, H.B. Balssall, W.R. Heineman, F.W. Scheller, Anal. Chem. 68 (1996) 2453–2458.
[36] H.J. Kim, J. Kwak, J. Electroanal. Chem. 577 (2005) 243–248.
[37] Y. Chen, W. Li, Y. Wang, X. Yang, J. Chen, Y. Jiang, C. Yu, Q. Lin, J. Mater. Chem. C 2 (2014) 4080–4085.
[38] J. Chen, H. Jiao, W. Li, D. Liao, H. Zhou, C. Yu, Chem. Asian J. 8 (2013) 276–281.